# Theoretical Study on Gold-Coated Iron Oxide Nanostructure: Magnetism and Bioselectivity for Amino Acids

**Q. Sun,*,†,‡ B.V. Reddy,§ M. Marquez,§,||,# P. Jena,‡ C. Gonzalez,|| and Q. Wang‡**

*Interdisciplinary Network of Emerging Science and Technologies, Research Center, Philip Morris USA, Richmond, Virginia 23234, Physics Department, Virginia Commonwealth University, Richmond, Virginia 23284, Research Center, Philip Morris USA, Richmond, Virginia 23234, NIST Center for Theoretical and Computational Nanosciences, National Institute of Standards and Technology, Gaithersburg, Maryland 20899P, and Harrington Department of Bioengineering, Arizona State University, Tempe, Arizona 85287*

*Received: October 29, 2006; In Final Form: January 22, 2007*

A fundamental understanding of the recent experiments of magnetic separation of amino acids using gold/iron oxide composite nanoparticles is provided for the first time by theoretically studying the interaction of gold-coated iron oxide cluster with sulfur-containing amino acids: cysteine, methionine, and taurine. We find, in agreement with experiments, that the interaction of cysteine is stronger than methionine, the interaction energies being 0.738 and 0.712 eV respectively. These energies are intermediate between van der Waals and covalent bonding and are ideal for effective binding and release in magnetic separation. On the other hand, we find that taurine, which is also a sulfur-containing amino acid, cannot bind to gold-coated iron oxide cluster. This selectivity can be used for the separation of taurine from the other two sulfur-containing amino acids. The present study provides insight on the mechanisms responsible for functionalizing iron oxide nanoparticles and may have far-reaching implications in biomedical research.

Recent studies suggest that magnetic nanoparticles can bind to bacteria,[1] protein,[2] and enzyme[3] and could be directed to an organ, tissue, or cancer tumor by using an external magnetic field.[4] Therefore, considerable experimental efforts have been devoted to the studies of biomedical applications of magnetic nanoparticles such as in magnetic resonance imaging contrast enhancement, tissue repair, immunoassay, detoxification of biological fluid, hyperthermia, targeted drug delivery, and cell separation.[5−7] Besides being small in size and biocompatible, a very basic requirement for enhanced application sensitivity entails high magnetization of the nanoparticle. For this reason, iron becomes a naturally preferred choice for fabricating such nanostructures.[8] From a practical point of view, however, iron nanoparticles are prone to easy oxidation. Some recent investigations even reveal that the previously claimed Fe-based structures are actually Fe-oxide-based.[9] Therefore, iron-oxide-based nanoparticles are extensively studied in synthesis for better control of size, shape, and composition.[10−19]

While the inherent magnetization is necessary for manipulation by an external field, the bare magnetic nanoparticles cannot be applied directly to the human body. A coating layer is needed to improve its biocompatibility, functionality, and stability. Gold is a widely used coating material because of its well-known advantages in biomedical applications.[20,21] Seino et al.[10] synthesized magnetic carriers consisting of nano iron oxide and gold core−shell structures in an aqueous solution by using $\gamma$-ray irradiation. Lyon et al.[11] prepared core−shell structures with gold coating layers on the surface of nanoparticles consisting of either $Fe_2O_3$ or partially oxidized $Fe_3O_4$ via iteration hydroxylamine seeding. They found a corresponding blue shift in the surface plasmon resonance. Yu et al.[12] also synthesized the so-called dumbbell-like Au−$Fe_3O_4$ bifunctional nanoparticles. Wang et al.[14] fabricated core (iron oxide)−shell (gold) nanocomposite and assembled into thin film materials by using presynthesized and size-defined iron oxide nanoparticles as seeding materials for the reduction of gold precursors. Furthermore, Seino and his collaborators[15] developed an original technique for immobilizing gold nanograins onto the surface of magnetic iron oxide nanoparticles, which enabled the binding of functional biomolecules possessing mercapto groups without using a special linker molecule. On the basis of this technique, Kinoshita et al.[16] carried out a study of the magnetic separation of amino acids by Au/Fe oxide composite nanoparticles. They found that among 17 amino acids used in experiment only two sulfur-containing amino acids (cystine and methionine) are adsorbed onto the gold-coated Fe oxide nanoparticles with the amounts of adsorbed sulfur-containing amino acids increasing with the Au wt % in the particles. Further, the adsorption of other amino acids decreased, suggesting that Au−S bonding is responsible for this behavior.

Despite the extensive experimental efforts, some basic questions still need to be addressed theoretically for improving design of such particles. (1) How does gold coating affect the structure and magnetism of the iron oxide core? (2) How strong is the interaction between amino acids and gold-coated iron oxide particles? If the interaction is too weak, the particles cannot be used as an effective carrier. On the other hand, if the binding is too strong, efficient release will remain a potential issue. Therefore, an effective separation requires that the bonding should be intermediate. (3) Although taurine was not tested in

* To whom correspondence should be addressed. E-mail: qsun@vcu.edu.
† Interdisciplinary Network of Emerging Science and Technologies, Research Center, Philip Morris USA.
‡ Virginia Commonwealth University.
§ Research Center, Philip Morris USA.
|| National Institute of Standards and Technology.
# Arizona State University.

10.1021/jp067095x CCC: $37.00 
Published on Web 02/27/2007

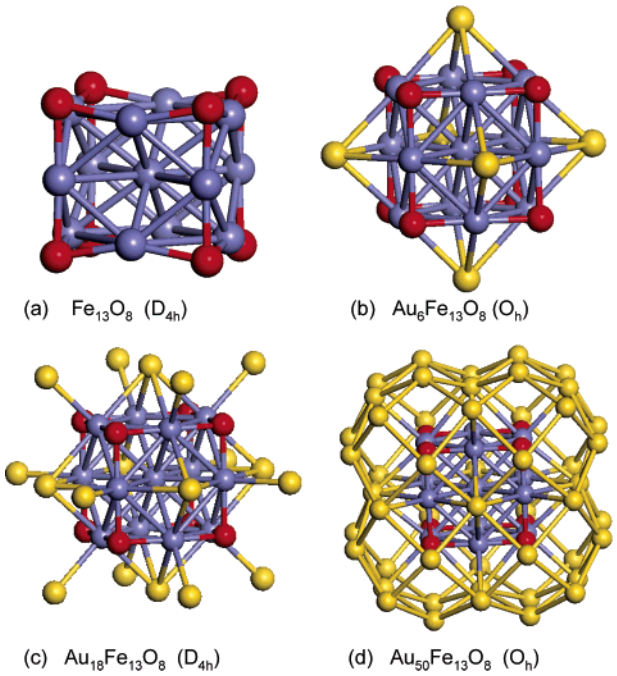


**Figure 1.** (Color online) (a) uncoated, (b, c) partially coated, and (d) fully coated gold−$Fe_{13}O_8$ clusters.

the experiment,[16] it is also a sulfur-containing amino acid. It would be very interesting to know if taurine also binds to the particle like cystine and methionine do.[4] Why does gold prefer to bind to sulfur-containing amino acids? In this paper, we present the first theoretical study that provides a fundamental understanding of these questions.

The oxidation of Fe is a very complicated process since different experimental conditions and environments yield varying stoichiometries in the composition of the samples. For example, the reported compositions in bulk are the well-known FeO, $Fe_2O_3$, $Fe_3O_2$, $Fe_3O_4$, or partially oxidized structures. The situation becomes even more complicated when dealing with clusters and nanoparticles of iron oxide with varying size and composition. Therefore, in this study, we consider a model system, namely, $Fe_{13}O_8$, which has been synthesized using a reactive laser-vaporized cluster source.[22] Mass spectrometric measurements indicate that this cluster exhibits a relatively high abundance in comparison with other iron oxide clusters with different compositions. In the above cluster, eight oxygen atoms are adsorbed on the surface of a $Fe_{13}$ cluster resulting in a structure with stable $D_{4h}$ symmetry,[22,23] as shown in Figure 1a. This cluster is used as a prototype for the iron oxide core to simulate gold-coated iron oxide core−shell structures, to study the changes in geometry and magnetism, and to explore its interactions with amino acids for understanding the recent experiments.[16]

Spin-polarized calculations of the total energies and forces on the basis of the density functional theory (DFT) were used to perform full geometry optimizations. We used a plane-wave basis set with the projector augmented plane wave (PAW) method as implemented in the Vienna ab initio Simulation Package (VASP).[24] All DFT calculations were performed with the generalized gradient approximation (GGA) for exchange-correlation functional developed by Perdew and Wang (PW91).[25,26] The geometries of the clusters were optimized without symmetry constraint using a conjugate-gradient search algorithm. We have used supercells with 14 Å vacuum spaces along the *x*, *y*, and *z* directions for all the calculated structures. The Γ point is used to represent the Brillouin zone because of the large supercell. The energy cutoff was set to 400 eV and the convergence in energy and force were $10^{-4}$ eV and $1 \times 10^{-3}$ eV/Å, respectively. The accuracy of our numerical procedure for $Fe_{13}O_8$ and gold nanostructures was well tested in our previous papers.[8,22,23,27,28]

Figure 1 shows the optimized structures of the uncoated (Figure 1a) and gold-coated (Figure 1b−d) $Fe_{13}O_8$ clusters considered in this study. A summary of our main results on the symmetry, magnetic moments, bond lengths, and coating energies per Au atom is given in Table 1. For all $Fe_{13}O_8$ clusters, the central Fe atom is labeled as Fe1, the surface Fe atom as Fe2, the corresponding magnetic moments as $\mu_{Fe1}$ and $\mu_{Fe2}$, and the average magnetic moment on Fe atom as $\mu_{Fe}$. First, we coated $Fe_{13}O_8$ with six Au atoms capping the six 4-fold sites (Figure 1b). Gold coating enlarges the Fe1−Fe2 and Fe2−Fe2 bond lengths to 2.612 and 2.613 Å, respectively, with a concomitant increase in the magnetic moment of the Fe sites ($\mu_{Fe1} = 2.915\ \mu_B$ and $\mu_{Fe2} = 2.676\ \mu_B$). In addition, the results in Table 1 show a slight spin polarization on the gold atoms ($0.087\ \mu_B$) and an average coating energy per Au atom (defined as $E = [E(Au_n{-}Fe_{13}O_8) - E(Fe_{13}O_8) - nE(Au)]/n$) of 2.463 eV.

Capping $Au_6{-}Fe_{13}O_8$ further with 12 gold atoms in an "on-top" approach to the surface Fe atoms results in the optimized $Au_{18}{-}Fe_{13}O_8$ cluster with $D_{4h}$ symmetry shown in Figure 1c. Although the bond lengths of Fe1−Fe2 and Fe2−Fe2 increased further to 2.645 and 2.646 Å, a net decrease in the average magnetic moment is observed ($2.356\ \mu_B$ vs $2.374\ \mu_B$ for $Fe_{13}O_8$ and $2.676\ \mu_B$ for $Au_6{-}Fe_{13}O_8$) mainly because of an increase in the coordination numbers. This decrease in the magnetic moments is accompanied by a significant decrease in average coating energy (1.61 eV vs 2.463 eV for $Au_6{-}Fe_{13}O_8$). To wrap $Fe_{13}O_8$ completely with a single gold shell, $Au_{18}Fe_{13}O_8$ needs to be capped with an additional 32 Au atoms. As shown in Figure 1d, the optimized structure of $Au_{50}Fe_{13}O_8$ has $O_h$ symmetry. The results listed in Table 1 indicate that the Fe1−Fe2 bond lengths in $Au_{50}Fe_{13}O_8$ are reduced to 2.605 Å. Despite this decrease in the Fe1−Fe2 bond length, the magnetic moment of Fe1 was found to increase ($2.788\ \mu_B$) because of the increased high symmetry of the cluster ($O_h$) as compared to $Au_{18}Fe_{13}O_8$ ($D_{4h}$). Although $Au_{50}Fe_{13}O_8$ and $Au_6Fe_{13}O_8$ exhibit the same $O_h$ symmetry, the Fe1−Fe2 distance in $Au_{50}Fe_{13}O_8$ is approximately 0.07 Å smaller than that in $Au_6Fe_{13}O_8$, leading to a smaller Fe1 magnetic moment in $Au_{50}Fe_{13}O_8$ These results lead to the conclusion that the magnetic moment on the central Fe1 atom is mainly controlled by symmetry and bond length. Capping $Au_{18}{-}Fe_{13}O_8$ with 32 Au atoms decreases the Fe2−Fe2 distance by 0.041 Å, which is accompanied by a corresponding decrease in the Fe2 magnetic moment of $0.071\ \mu_B$

**TABLE 1: Symmetry (sym), Magnetic Moment $\mu$ (in $\mu_B$), Bond Length *R* (in Å), and Coating Energy *E* per Au Atom (in eV) for the Studied Clusters**

| | sym | $\mu_{Fe1}$ | $\mu_{Fe2}$ | $\mu_{Fe}$ | $\mu_{Au}$ | $R_{Fe1-Fe2}$ | $R_{Fe2-Fe2}$ | $R_{Fe2-O}$ | $R_{Fe2-Au}$ | E |
|---|---|---|---|---|---|---|---|---|---|---|
| $Fe_{13}O_8$ | $D_{4h}$ | 2.797 | 2.339 | 2.374 | | 2.496 | 2.345 | 1.877 | | |
| $Au_6{-}Fe_{13}O_8$ | $O_h$ | 2.915 | 2.676 | 2.694 | 0.087 | 2.612 | 2.613 | 1.875 | 2.666 | 2.463 |
| $Au_{18}{-}Fe_{13}O_8$ | $D_{4h}$ | 2.600 | 2.336 | 2.356 | 0.036 | 2.645 | 2.646 | 1.838 | 2.592 | 1.610 |
| $Au_{50}{-}Fe_{13}O_8$ | $O_h$ | 2.788 | 2.265 | 2.305 | 0.019 | 2.605 | 2.605 | 1.817 | 2.665 | 1.669 |

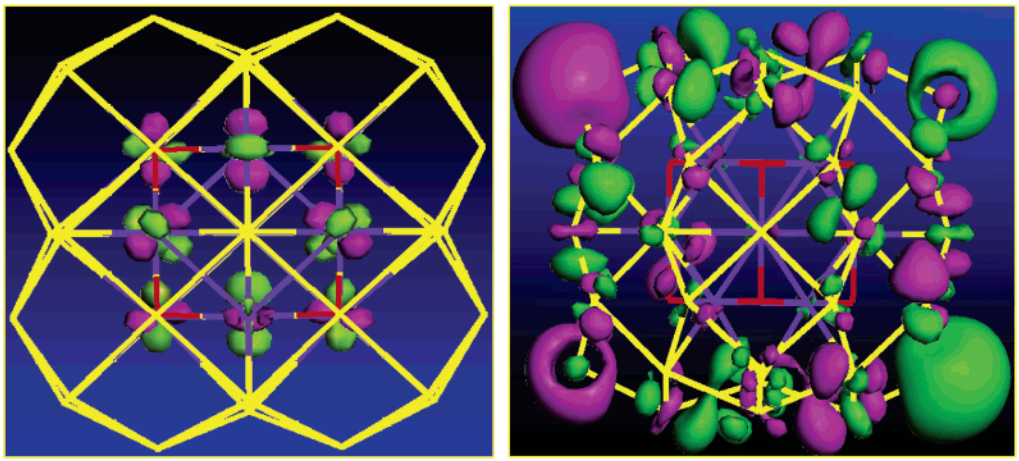


**Figure 2.** (Color online) HOMO (a) and LUMO (b) of $Au_{50}Fe_{13}O_8$.

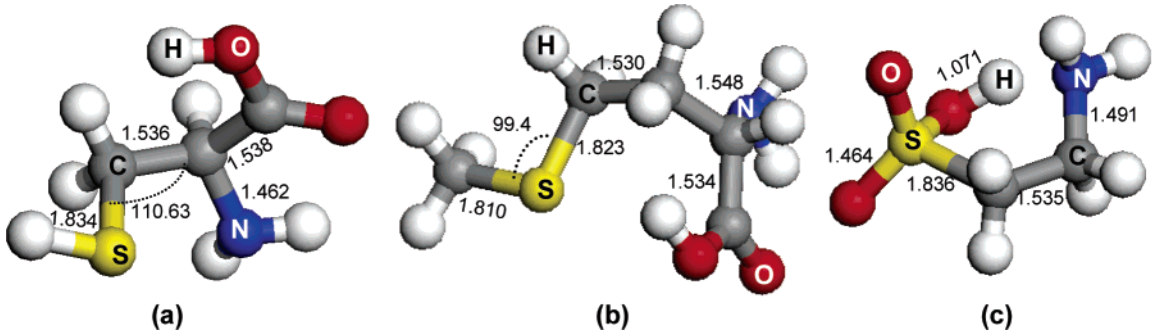


**Figure 3.** (Color online) Geometry of cysteine (a), methionine (b), and taurine (c).

(Table 1). Nevertheless, it is very encouraging to note that in this completely coated iron oxide cluster, the average magnetic moment on the Fe sites is 2.305 $\mu_B$, still larger than that of the value in bulk Fe (2.20 $\mu_B$). Therefore, gold coating can keep the magnetism alive, thus providing the basis for the applications of gold-coated iron oxide nanoparticles in magnetic drug delivery and magnetic fluid hyperthermia, as discussed above. Furthermore, the changes in the average moment on Fe site (see the fifth column in Table 1) suggest that the magnetic moment is not very sensitive to gold coating. This is in agreement with experimental finding that magnetic properties remain largely independent of Au addition.[11] In Figure 2, we show the highest occupied molecular orbital (HOMO) and the lowest unoccupied molecular orbital (LUMO) for this completely coated iron oxide cluster ($Au_{50}Fe_{13}O_8$). It clearly indicates that the HOMO is mainly contributed by the d-orbitals of Fe atom in the core part, while the LUMO is predominantly associated with the gold-coating shell.

So far, the results of our calculations regarding the changes in geometry and magnetism upon gold coating of $Fe_{13}O_8$ clusters can be summarized as follows: (1) Gold coating expands the geometry of the iron oxide core resulting in larger Fe−Fe bond lengths, however, the magnetic moments on Fe sites are determined by a delicate balance between symmetry, bond length, and coordination. (2) The magnetism is not very sensitive to gold coating. (3) The gold atoms get polarized with small magnetic moments, but as more Au atoms are added, the induced moment decreases because of an increase in the Au−Au interactions.

Recent experiments[16] suggest that gold-coated iron oxide nanoparticles can effectively bind with some sulfur-containing amino acids such as cystine and methionine. These amino acids are responsible for some important biological functions: Cysteine assists tissues damaged by alcohol abuse, cigarette smoke, and air pollution through the detoxification of acetaldehyde. Methionine is a naturally occurring amino acid, which is an essential component of the diet, furnishing both sulfur and methyl groups necessary for the normal metabolic function. It can assist in the removal of toxic wastes from the liver and prevents deposits and cohesion of fats in the liver. Besides cystine and methionine, another sulfur-containing amino acid is taurine. As a nutrient, it protects the cell membranes by attenuating such toxic compounds as oxidants, secondary bioacids, and antibiotics. The results of the experimental work[16] have prompted the following questions: Out of the three sulfur-containing amino acids, cysteine ($H_7C_3NO_2S$, two molecules of cysteine make cystine), methionine ($H_{11}C_5NO_2S$), and taurine ($H_7C_2NO_3S$), why is cystine more populated than methionine when binding to gold-coated iron oxide nanoparticles? Can taurine also bind to the particle? In the following, we use the partially coated $Au_6Fe_{13}O_8$ cluster as a prototype to address these questions. Although $Au_{50}Fe_{13}O_8$ is fully coated, it is difficult to study its binding with amino acids for the following reason: It exhibits low symmetry with four nonequivalent positions for gold atoms. These four sites contain 6, 8, 12, and 24 Au atoms, respectively. By contrast, the $Au_6Fe_{13}O_8$ structure contains six equivalent gold atoms, which makes the study of the binding of amino acids very tractable from the computational point of view.

Figure 3 shows the optimized structures of the amino acids cysteine, methionine, and taurine, while the optimized structures of cysteine and methionine bonded to $Au_6Fe_{13}O_8$ are shown in Figure 4 (the structure of $Au_6Fe_{13}O_8$ is also shown for comparison). The results of our calculations indicate that the

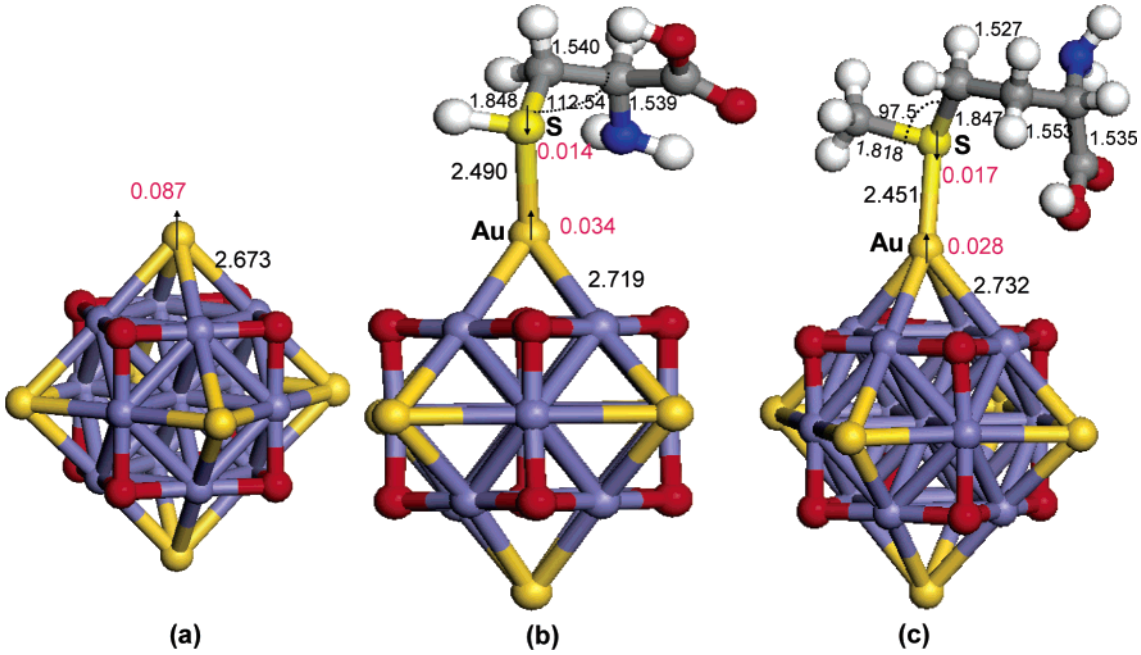


**Figure 4.** (Color online) Geometry of $Au_6Fe_{13}O_8$ (a), cysteine−$Au_6Fe_{13}O_8$ (b), and methionine−$Au_6Fe_{13}O_8$ (c). The numbers close to arrows correspond to the spins on Au and S atoms while the other numbers correspond to bond lengths and bond angles.

binding between cysteine and $Au_6Fe_{13}O_8$ is characterized by a Au−S distance of 2.490 Å (Figure 3b), interaction energy of 0.738 eV, and a net transfer of approximately 0.2 electrons from S to Au. No significant changes in the geometry of the cysteine fragment were observed. In addition, the calculations predict an overall enlargement of the Au−Fe bond length (2.719 Å vs 2.673 Å, see Figure 4) when compared to the bare $Au_6Fe_{13}O_8$ cluster as a result of the Au−cysteine interaction. The induced magnetic moment on Au atom was reduced to 0.034 $\mu_B$ from its original value of 0.087 $\mu_B$ in the bare $Au_6Fe_{13}O_8$ cluster, while the S atom was antiferromagnetically polarized with a small moment of 0.014 $\mu_B$. The adsorption profile of methionine on $Au_6Fe_{13}O_8$ is very similar to the one obtained in the case of cysteine with no significant structural changes in the amino acid. The Au−S distance is 2.451 Å and the interaction energy is 0.712 eV with a partial charge transfer of 0.1 electrons from S to Au. As with the case of cysteine, a slight enlargement (0.059 Å) of the Au−Fe bond length as compared to the bare cluster was found (see Figure 4).

As previously discussed, experimental evidence suggests that the population of cystine bound to gold-coated iron oxide is more than that of methionine. Our theoretical results predict that absorption of cysteine to the gold-coated iron oxide is accompanied by a somewhat larger electron transfer and larger binding energy than the corresponding adsorption of methionine to the same cluster. Given that the actual amino acid used in the experiment was cystine that consists of two cysteines, it is understandable that, because of two sulfur atoms, the population of cystine-gold-coated iron oxide is larger than that of methionene. However, in the case of taurine, the S atom is already bound to three O atoms and one C atom (see Figure 3c), and thus, it would possibly make the Au−S binding difficult. In fact, our calculations find no evidence for taurine binding to $Au_6Fe_{13}O_8$ through the Au−S contact, and gold-coated iron oxide particles are not good taurine carriers. This confirms the expectation that high oxidation state of sulfur is not able to form a stable bond with gold.

**TABLE 2: Comparisons of Atomic Levels (in eV)**[a]

| Au 6s5d | S 3p | B 2p | C 2p | N 2p | O 2p | P 3p | Si 3p |
|---|---|---|---|---|---|---|---|
| ↑ ↓ | ↑ ↓ | ↑ ↓ | ↑ ↓ | ↑ ↓ | ↑ ↓ | ↑ ↓ | ↑ ↓ |
| -6.08 (6s) | | -4.01 | | | | | -4.35 |
| -6.73 (5d) | -6.01 | | -6.12 | | | -6.21 | |
| -7.02 (5d) | -7.68 | | | -8.29 | -7.22 | | |

[a] Arrows specify spin-up and spin-down.

Finally, we return to the question concerning why the strength of the Au−S bonding seems to be an important factor controlling biolabeling and separation. The relatively large affinity of gold toward sulfur can be rationalized on the basis of an analysis of the atomic energy level diagram shown in Table 2. Compared to other atoms such as B, C, N, O, P, and Si, the 3p energy level in S is significantly closer to the 6s orbital energy in Au, which makes the Au−S bonding more favorable. This is one of the reasons why thiolates and thiols are widely used to functionalize gold in chemistry, chemical engineering, and molecular electronics.[29,30] Since the human body contains sulfur (mainly in the proteins distributed in all cells and tissues) and can easily bind to gold (which is biocompatible) for functionalization, this provides a substantial basis for using gold-coated magnetic nanostructures in labeling, targeting, separation, and drug delivery.

There are some potential issues that need to be addressed. For example, what is the effect of core size of iron oxide and the gold-coating layers on the magnetic moment of the particles? The present computational limitations, unfortunately, do not permit us to study the effect of gold-coating layers and core size. However, similar calculations carried out by us on gold-coated Fe clusters[8] reveal that the magnetic moments are not sensitive to the number of gold layers while they slowly decrease as the surface-to-volume ratio decreases. A single layer of gold coating is, indeed, enough to render the particle chemical inertness and biocompatibility. Excessive coating by gold may hinder the radio frequency to penetrate into the particle and, hence, may adversely affect their applicability for magnetic fluid hyperthermia. So, in experiment, only a very thin gold shell is coated to avoid this problem.

In summary, we present the first theoretical study leading to a fundamental understanding of the interaction of amino acids with gold-coated iron oxide particles and the effect of gold coating on the magnetic moments of the iron oxide core. We show that gold coating preserves the magnetic property of the iron core while enhancing its stability. The gold-coated iron oxide particle can selectively bind with sulfur-containing amino acids. The combination of magnetism, selectivity, and stability displayed in gold-coated iron oxide particle makes it very promising for applications such as in magnetic separation, controlled release, and targeted drug delivery.

**Acknowledgment.** Q. Sun thanks Dr. M. Hajaligol for stimulating discussions.

## References and Notes

(1) Matsunaga, T.; Okamura, Y.; Tanaka, T. *J. Mater. Chem.* **2004,** *14*, 2099.

(2) Bucak, S.; Jones, D. A.; Laibinis, P. E.; Hatton, T. A. *Biotechnol. Prog.* **2003,** *19*, 477.

(3) Koneracka, M.; Kopcansky, P.; Timko, M.; Ramchand, C. N. *J. Magn. Magn. Mater*. **2002**, *252*, 409.

(4) Forbes, Z. G.; Yellen, B. B.; Barbee, K. A.; Friedman, G. *IEEE Trans. Magn.* **2003,** *39*, 3372.

(5) Tartaj, P.; Morales, M.; Verdaguer, S. V.; Carreño, T. G.; Serna, C. J. *J. Phys. D: Appl. Phys.* **2003,** *36*, R182.

(6) Pankhurst, Q. A.; Connolly, J.; Jones, S. K.; Dobson J. *J. Phys. D: Appl. Phys.* **2003,** *36*, R167.

(7) Mornet, S.; Vasseur, S.; Grasset, F.; Duguet, E. *J. Mater. Chem.* **2004,** *14*, 2161.

(8) Sun, Q.; Kandalam, A. K.; Wang, Q.; Jena, P.; Kawazoe, Y.; Marquez, M. *Phys. Rev. B* **2006,** *73*, 134409.

(9) Rave, B.; Carpenter, E. E.; Harris, V. G. *J. Appl. Phys*. **2002,** *91*, 8195.

(10) Seino, S.; Kinoshita, T.; Otome, Y.; Nakagawa, T.; Okitsuc, K.; Mizukoshid, Y.; Nakayama, T.; Sekino, T.; Niihara, K.; Yamamoto, T. A. *J. Magn. Magn. Mater*. **2005,** *293*, 144.

(11) Lyon, J. L.; Fleming, D. A.; Stone, M. B.; Schiffer, P.; Williams, M. E. *Nano Lett.* **2004,** *4*, 719.

(12) Yu, H.; Chen, M.; Rice, P. M.; Wang, S. X.; White, R. L.; Sun, S. *Nano Lett*. **2005,** *5*, 379.

(13) Wang, L.; Luo, J.; Maye, M. M.; Fan, Q.; Rendeng, Q.; Engelhard, M. H.; Wang, H.; Lin, Y.; Zhong, C. J. *J. Mater. Chem.* **2005,** *15*, 1821.

(14) Wang, L.; Luo, J.; Fan, Q.; Suzuki, M.; Suzuki, I. S.; Engelhard, M. H.; Lin, Y.; Kim, N.; Wang, J. Q.; Zhong, C. J. *J. Phys. Chem. B* **2005,** *109*, 21593.

(15) Seino, S.; Kinoshita, T.; Otome, Y. *Chem. Lett*. **2003,** *32*, 690.

(16) Kinoshita, T.; Seino, S.; Mizukoshi, Y.; Otomea, Y.; Nakagawa, T.; Okitsud, K.; Yamamoto, T. A. *J. Magn. Magn. Mater*. **2005,** *293*, 106.

(17) Seino, S.; Kusunose, T.; Sekino, T.; Kinoshita, T.; Nakagawa, T.; Kakimi, Y.; Kawabe, Y.; Lida, J. J.; Yamamoto, T. A.; Mizukoshi, Y. *J. Appl. Phys*. **2006**, *99*, 08H101.

(18) Lu, Q. H.; Yao, K. L.; Xi, D.; Liu, Z. L.; Luo, X. P.; Ning, Q. *J. Magn. Magn. Mater*. **2006**, *301*, 44.

(19) de la Fuente, J. M.; Alcantara, D.; Eaton, P.; Crespo, P.; Rojas, T. C.; Fernandez, A.; Hernando, A.; Penades, S. *J. Phys. Chem. B* **2006**, *110*, 13021.

(20) Shukla, R.; Bansal, V.; Chaudhary, M.; Basu, A.; Bhond, R. R.; Sastry, M. *Langmuir* **2005**, *21*, 10644.

(21) Sun, Q.; Wang, Q.; Rao, B. K.; Jena, P. *Phys. Rev. Lett.* **2004**, *93*, 186803.

(22) Wang, Q.; Sun, Q.; Sakurai, M.; Yu, J. Z.; Gu, B. L.; Sumiyama, K.; Kawazoe, Y. *Phys. Rev. B* **1999**, *59*, 12 672.

(23) Sun, Q.; Wang, Q.; Parlinski, K.; Yu, J. Z.; Hashi, Y. Gong, G. X.; Kawazoe, Y. *Phys. Rev. B* **2000**, *61*, 5781.

(24) Kresse, G.; Furthmüller, J. *Phys. Rev. B* **1996**, *54*, 11169.

(25) Becke, A.D. *Phys. Rev. A* **1988**, *38*, 3098.

(26) Perdew, J. P.; Wang, Y. *Phys. Rev. B* **1992**, *45*, 13244.

(27) Sun, Q.; Wang, Q.; Jena, P.; Note, R.; Yu, J.-Z.; Kawazoe, Y. *Phys. Rev. B* **2004**, *70*, 245411.

(28) Sun, Q.; Wang, Q.; Kawazoe, Y.; Jena, P. *Eur. Phys. J. D* **2004**, *29*, 231.

(29) Love, J. C.; Estroff, L. A.; Kriebel, J. K.; Nuzzo, R. G.; Whitesides, G. M. *Chem. Rev*. **2005**, *105*, 1103.

(30) Daniel, M. C.; Astruc, D. *Chem. Rev*. **2004**, *104*, 293.